Magnetic circular dichroism spectra in a II-VI diluted magnetic semiconductor $Zn_{1-x}Cr_xTe$: First-principles calculations

Hongming Weng,[1,*] Jinming Dong,[2] Tomoteru Fukumura,[1] Masashi Kawasaki,[1] and Yoshiyuki Kawazoe[1]
[1]*Institute for Materials Research, Tohoku University, 2-1-1 Katahira, Aoba-ku, Sendai 980-8577, Japan*
[2]*Group of Computational Condensed Matter Physics, National Laboratory of Solid State Microstructure and Department of Physics, Nanjing University, Nanjing 210093, People's Republic of China*
(Received 15 May 2006; revised manuscript received 17 July 2006; published 6 September 2006)

The absorption and magnetic circular dichroism (MCD) spectra of $Zn_{1-x}Cr_xTe$ for $x=0.0625$, 0.25, and 1.0 are studied using the first-principles method. The calculated MCD spectra are found to be well consistent with the experimental measurement at the L critical points (CPs) in spite of opposite MCD sign at absorption edge E_0 between calculation and experiment. The MCD signals at these CPs indicate that in $Zn_{1-x}Cr_xTe$ the p-d exchange interaction does exist and it is ferromagnetic. The MCD spectrum of NiAs-type CrTe is also calculated, which is comparable with the experimental one and totally different from that of $Zn_{1-x}Cr_xTe$. All of these results show that the MCD spectra of diluted magnetic semiconductor (DMS) do originate from its band structure and the MCD analysis is efficient in identifying the p-d exchange interaction in it and can be used for discriminating between DMS and other magnetic precipitates in samples.

DOI: 10.1103/PhysRevB.74.115201 PACS number(s): 75.50.Pp, 75.30.Et, 78.20.Ls

I. INTRODUCTION

Ferromagnetic (FM) diluted magnetic semiconductors (DMSs), especially those having room-temperature (RT) ferromagnetism, have attracted great interest from researchers due to their potential applications in spintronic devices.[1] Many systems, such as GaN:Mn (Ref. 2), GaN:Cr (Ref. 3), TiO_2:Co (Ref. 4), ZnO:Co (Ref. 5), ZnO:Mn (Ref. 6), $CdGeP_2$:Mn (Ref. 7), and ZnTe:Cr (Ref. 8 and 9) have been reported to have RT ferromagnetism. Lots of magnetization measurements and crystallographic studies have been intensively performed, trying to conclude the ferromagnetism in these materials is from the expected DMS, but there are still controversies on whether the observed ferromagnetism comes from the DMS or other magnetic precipitates. To resolve such a problem, experimental measurement of the magnetic circular dichroism (MCD) spectra is needed, which is thought to be one of three efficient methods to identify the intrinsic FM DMS (Ref. 10 and 11). The most studied DMS systems are characterized by the s, p-d exchange interaction between the s, p bands of a host semiconductor and the d local states of the transition metal dopant,[12,13] which induces giant Zeeman splitting in the s, p bands of the host, leading to quite large magneto-optical (MO) effects. Therefore, the experimental measurements of the MO effects, especially the MCD spectra, play an important role in clarifying the s, p-d exchange interaction and the electronic structures of DMSs.[13] For example, the MCD measurements have confirmed that s, p-d exchange interaction does exist in GaAs:Mn (Ref. 14), GaN:Mn (Ref. 15), GaAs:Cr (Ref. 16), InAs:Mn (Ref. 17), ZnTe:Cr (Ref. 8), and ZnO:Co (Ref. 18 and 19). In addition, further MCD analysis clarified that only GaAs:Mn, InAs:Mn, and ZnTe:Cr are intrinsic FM DMSs, while ZnO:TM (TM=Mn, Fe, Co, Ni, or Cu), GaN:Mn and GaAs:Cr are paramagnetic although they have an s, p-d exchange interaction.[19]

Despite these intense experimental efforts, up to now, theoretical studies, especially the *ab initio* calculations of MCD spectrum in DMS are still very few although they are urgently needed for identifying the experimentally observed MCD signals and justifying the capability of this method in estimation of the s, p-d exchange interaction.[11,20] A clear correspondence between the shape of the FM MCD spectra and the expected band structure is needed. For this purpose, in this paper, we have performed an accurate study of MCD spectra by band structure calculations. The Cr-doped ZnTe ($Zn_{1-x}Cr_xTe$) is taken as an example to show how efficient the approach is since it is one of the traditional zinc-blende (ZB) II-VI DMS, a prototype of many other DMSs, and also the experimental MCD analysis shows it is a RT FM DMS (Ref. 8).

II. METHODOLOGY

The highly accurate all electron full-potential linearized augmented plane-wave method implemented in WIEN2K (Ref. 21) is used for electronic structure calculation within the generalized gradient approximation (GGA).[22] To simulate the doping concentration of $x=0.0625$ and 0.25, one apical Zn atom is replaced by Cr in a $\sqrt{2}\times\sqrt{2}\times 2$ and $1\times 1\times 1$ supercell of the ZB phase ZnTe, respectively. The spin-orbit coupling (SOC) is taken into account with the magnetization aligned along [001] directions by using the second-variation method[23] self-consistently. The optical conductivity $\sigma_{\alpha\beta}$ $(\alpha,\beta\equiv x,y,z)$ is calculated within the electric-dipole approximation using the well-known Kubo linear-response formula: (Refs. 24 and 25),

$$\sigma_{\alpha\beta}(\omega)=\frac{ie^2}{m^2\hbar V}\sum_k\sum_{j,j'}\frac{f(E_{jk})-f(E_{j'k})}{\omega_{jj'}}\left[\frac{\Pi^{\alpha}_{j'j}\Pi^{\beta}_{jj'}}{\omega-\omega_{jj'}+i/\tau}+\frac{(\Pi^{\alpha}_{j'j}\Pi^{\beta}_{jj'})^*}{\omega+\omega_{jj'}+i/\tau}\right]. \quad (1)$$

Here, $f(E_{jk})$ is the Fermi function, $\hbar\omega_{jj'}=E_{jk}-E_{j'k}$ is the

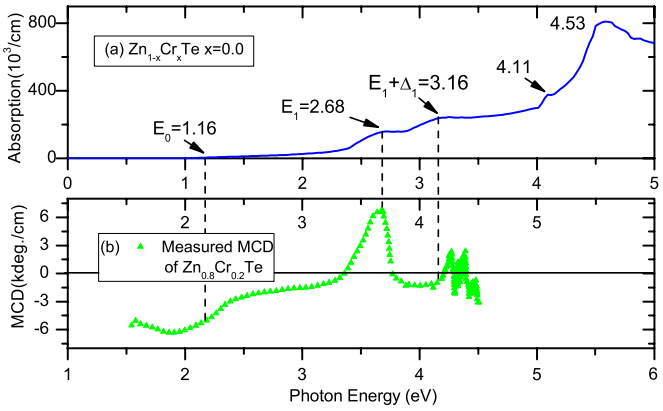

FIG. 1. (Color online) (a) The absorption spectrum of pure ZnTe calculated with $\hbar/\tau=0.0$. E_0, E_1, $E_1+\Delta_1$, and other CPs are indicated by the numbers (in eV) nearby the peaks. (b) The MCD spectrum of a 80-nm thick $Zn_{1-x}Cr_xTe$ ($x=0.20$) film on ZnTe buffer with several monolayers measured in Ref. 8. The x axis starts from 1.0 eV and the vertical dashed lines indicate the positions of CPs.

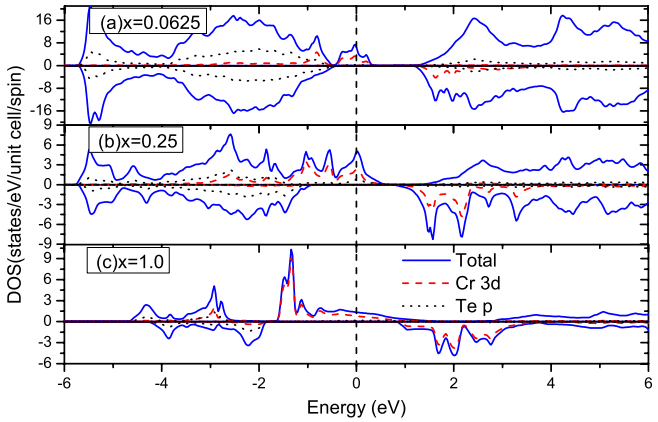

FIG. 2. (Color online) The total (solid line), projected Cr $3d$ (dashed line) and Te p (dotted line) DOS for (a) $x=0.0625$, (b) $x=0.25$, and (c) $x=1.0$. The vertical dashed line indicates the Fermi level. The positive (negative) DOS value represents the majority (minority) spin channel.

energy difference of the Kohn-Sham energies E_{jk}, and τ^{-1} is the inverse of the lifetime of excited Bloch electron states, the only parameter used in the whole calculation. $\Pi^{\alpha}_{j'j}$ is the element of the dipole optical transition matrix. The upper limit of the band index j and j' is taken as the band lying at as high as 2.5 Ry above Fermi level, and the convergence is carefully checked by varying it from 1.5 to 3.5 Ry. Totally, 20 000 k points are sampled in the Brillouin zone of the conventional ZB unit cell for the integral of k space. The convergence is carefully checked. Once the optical conductivity elements are obtained, the right- (α^+) and left- (α^-) circular polarized absorption is calculated by $\alpha^{\pm} \approx 4\pi * \mathrm{Re}(\sigma_{xx} \pm i\sigma_{xy})/c$ with c as the speed of light.[26]

III. RESULT AND DISCUSSION

At first, let us look at the calculated critical points (CPs) in the absorption spectrum of pure ZnTe. To clearly show each CP, $\hbar/\tau=0.0$ is used in the calculation of Fig. 1(a). $E_0=1.16$ eV is the absorption edge due to the direct band gap transition at Γ point. The two L-CPs, E_1 at 2.68 eV and $E_1+\Delta_1$ at 3.16 eV, are from the transitions at the L point, where SOC lifts the degeneracy of light and heavy hole bands by a gap of Δ_1. The other CPs are contributed by other band transitions.[27] All of the obtained CPs are lower than the experimental values by about 1.0 eV since the the energy gap is underestimated, which is a well-known shortcoming of GGA (Ref. 28). The experimental absorption edge E_0 is around 2.4 eV and E_1, $E_1+\Delta_1$ is 3.7, 4.2 eV, respectively.[8] CPs form a fingerprint for each material. According to them, the material responsible for the observed MCD can be identified, which is shown by plotting the experimentally measured MCD spectrum of $Zn_{1-x}Cr_xTe$ with $x=0.20$ (Ref. 8) in Fig. 1(b). Note that the x axis of MCD spectrum starts from 1.0 eV in order to match the CPs indicated by the vertical dashed lines. Obviously, the observed MCD spectra are correlated well with the CPs, indicating that the sample has the similar band structure of ZnTe and s, p-d exchange interaction exists. The measured MCD is negative around E_0 and has opposite signs at L-CPs, positive at E_1 and negative at $E_1+\Delta_1$. For higher photon energy, the signal is illegible or not available in the measurement due to the strong absorption.[8]

When Cr is doped into ZnTe, the local d obitals of the Cr atom are introduced into the gap of ZnTe as shown by the total and projected Cr $3d$ density of states (DOS) in Fig. 2, which also indicates that $Zn_{1-x}Cr_xTe$ is half metallic in all the nonzero doping concentration studied here. The local magnetic moment on Cr atom is about 3.61 to 3.76 μ_B. These results are nearly the same as those in Refs. 25 and 29. It is noticed that the host's valence band maximum composed of Te p bands is lower than the localized Cr $3d$ orbitals, and the spin splitting in them due to the p-d exchange interaction is also obvious. This picture of energy level has already been intensively discussed in Refs. 25 and 30. According to the Schrieffer-Wolff formula and the spin splitting of Te p bands,[13,25,30,31] the sign of p-d exchange interaction in these systems is estimated to be positive.

The direct result of s, p-d exchange interaction is the strong MO effects in DMS. It is well known that MCD signal at E_0 and E_1 is proportional to $x(N_0\beta - N_0\alpha)\langle S_z\rangle dR/dE$ and $x\left(\frac{1}{4}N_0\beta - N_0\alpha\right)\langle S_z\rangle dR/dE$, respectively. The signal at $E_1+\Delta_1$ is always opposite to that at E_1.[13,30] Here, x is doping concentration and $N_0\alpha$ ($N_0\beta$) is the s-d (p-d) exchange integral between the conduction (valence) band and the Cr $3d$ orbital. $\langle S_z\rangle$ is the average spin component of the magnetic ion along the direction of external field, which is taken as positive. R is the absorption coefficient and E is the photon energy. dR/dE is found to be positive at E_0, E_1, and $E_1+\Delta_1$. It is known that in the ZB phase, the p-d exchange interaction is mostly contributed by the hybridization of p, d wave functions, while the s-d exchange interaction comes from the Coulomb interaction, which means that $N_0\alpha$ is always positive and smaller than $N_0\beta$ in magnitude.[13] According to these arguments, the positive (negative) MCD signal at E_0, or positive (negative) one at E_1 accompanied by an opposite signal at $E_1+\Delta_1$, indicates that $N_0\beta$ is positive (negative), i.e., the p-d exchange

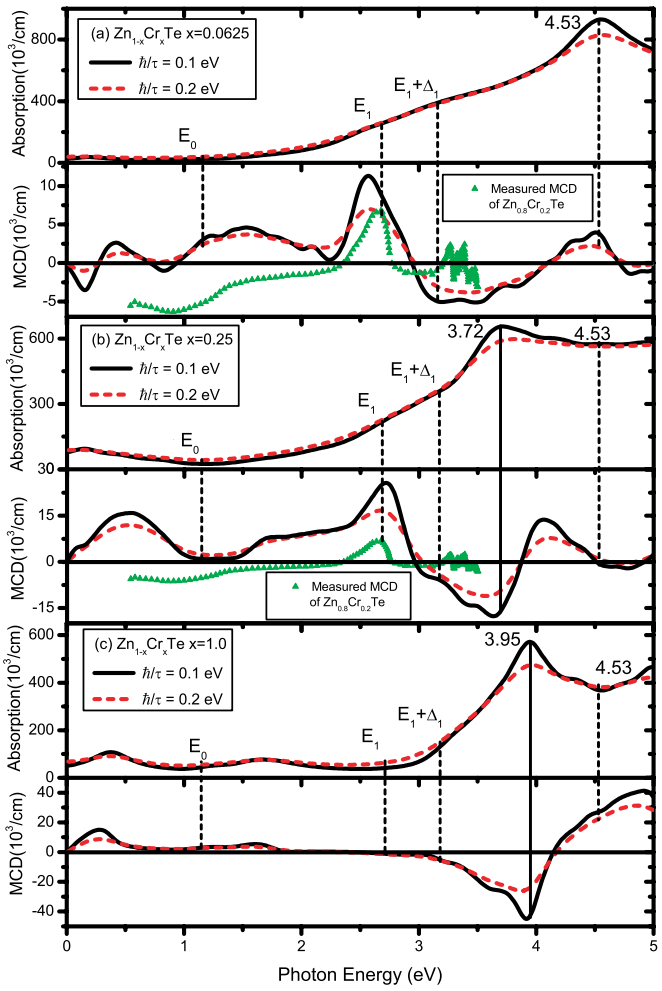

FIG. 3. (Color online) Calculated absorption and MCD spectra for (a) $x=0.0625$, (b) $x=0.25$, and (c) $x=1.0$ with $\hbar/\tau=0.1$ (solid line), 0.2 (dashed line) eV. The CPs at E_0, E_1 and $E_1+\Delta_1$, and 4.53 eV are indicated by the vertical dashed lines. The vertical solid line indicates the peaks that appear in the high x case. Experimental MCD spectrum in Fig. 1(b) is also shown for easy comparing.

interaction is FM (antiferromagnetic).[8,13,14] Therefore, MCD study has advantages in identifying the s,p-d exchange interaction in DMS over other magnetization or crystallographic measurements.[19]

The calculated absorption and MCD spectra for $x=0.0625$, 0.25, and 1.0 are presented in Fig. 3. In the low concentration case of $x=0.0625$, comparing the absorption spectrum with that of the pure case, it seems that the sparsely doped Cr $3d$ states only have contributions to the small in-gap absorption by keeping the whole shape and CPs of the absorption spectrum nearly unaffected. In fact, additionally, the local moment of Cr $3d$ states induces quite large Zeeman splitting in the host bands, which is clearly reflected by the MCD spectrum. As shown in Fig. 3(a), at the E_0 CP, the calculated MCD is positive, which is different from the experimental one. While at the two L-CPs, a positive MCD signal at E_1 and a negative one at $E_1+\Delta_1$ are obtained, which is consistent with the general characteristics of the Zeeman splitting induced by the s,p-d exchange interaction as discussed above and reproduces the experimental spectrum very well. This characteristic MCD structure corresponds to the FM p-d exchange interaction, in accord with the calculated positive MCD signal at the E_0 point. We noticed that the main qualitative properties of these critical MCD signals would not change with the relaxation time parameter $\hbar/\tau$, although some finer structures will disappear or be smoothed as $\hbar/\tau$ increases as shown in Fig. 3. The MCD signal at 4.53 eV is positive, but in the experimental measurement this signal is not available due to the strong absorption of light.

One of the stark contrasts to the experimental MCD is the sign at E_0 point. Though in experiment the negative MCD signal at E_0 point had been carefully studied and concluded to be from the $Zn_{1-x}Cr_xTe$ DMS, $N_0\beta$ estimated from this MCD signal would be negative, contrary to that reflected by the MCD structure at E_1 and $E_1+\Delta_1$. In our calculation, the consistence of $N_0\beta$ is well kept. In fact, there are many factors to affect the sign of MCD around E_0, e.g., the carrier concentration, the electronic state, and distribution of the doped ions.[32] Changes of one of them might reverse the MCD signal at E_0 since the transitions between the bands near the Γ point would become quite complex once the local d orbitals, s,p-d exchange interaction and Moss-Burstein shift are introduced.[32] In our calculation, there are no additional carriers introduced and the Cr ions are in the +2 state and uniformly distributed within the substitutional supercell approximation, while in the experimental measurement, the p-type samples are used.[8] It is believed that the transitions at L-CPs are not so much affected by these factors because the large dispersion of the s and p bands in the ZB phase makes them far from the bottom and top of the conduction and valence bands, respectively. Therefore, the MCD signals around L-CPs are much more stable and more reliable than that at E_0, and the above model formula explanation is applicable at L-CPs but should be carefully used at the E_0 point.[32]

As x is increased to 0.25, close to the experimental case of $x=0.20$, the in-gap absorption is a little larger due to more in-gap Cr $3d$ bands compared with the case of $x=0.0625$. The weight of transitions from Te p to Cr $3d$ is also increased, which contributes to the absorption peak and corresponding negative MCD signal at about 3.72 eV as indicated by the vertical solid line in Fig. 3(b). The CPs from the host ZnTe still exist and the signs of corresponding MCD are kept as the same as those in $x=0.0625$ although the magnitude is larger now. It is obvious that the critical features of the MCD would not change with the doping concentration in the studied region ($x\leqslant 0.25$), which is consistent with the x dependence of the MO Kerr effects in $Ga_{1-x}Mn_xAs$.[33]

When Cr fully substitutes Zn at $x=1.0$, the CPs originating from the transitions of Te p to Zn $4s$ will disappear. Instead, the transitions from Te p to Cr $3d$ and $4s$ will dominate the absorption and MCD spectra. The absorption peak around 3.95 eV resembles that around 3.72 eV at $x=0.25$ because both are contributed to by the transitions from Te p to Cr $3d$ bands, which is clearly shown by more detailed band-structure analysis in Ref. 25 and DOS in Fig. 2. Due to the absence of Zn $4s$ conduction bands, a vale instead of a peak appears around 4.53 eV. Although the positive MCD still exists around the E_0, the characteristic MCD structures around E_1 and $E_1+\Delta_1$ CPs disappear. The MCD intensity

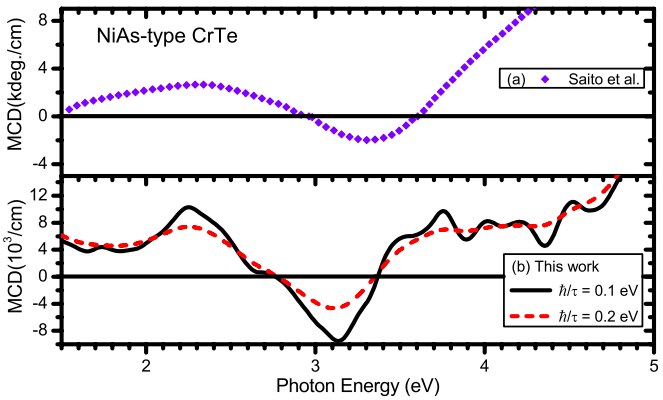

FIG. 4. (Color online) (a) Measured (Ref. 8) and (b) calculated MCD spectrum of NiAs-type CrTe. In the calculation, $\hbar/\tau$ is taken as 0.1 (solid line), 0.2 (dashed line) eV.

around 4.0 eV is enhanced compared to that in the case of $x=0.25$ due to the increased weight of the Cr $3d$ bands.

In the experimental samples of $Zn_{1-x}Cr_xTe$, the most possible magnetic precipitate is the hexagonal NiAs-type CrTe (h-CrTe).[8] To confirm the RT FM samples are free of *h*-CrTe, the MCD spectrum of *h*-CrTe is measured and found to be totally different from that of $Zn_{1-x}Cr_xTe$. The measured and calculated MCD spectra of *h*-CrTe are shown in Fig. 4. Given the fact that a 10-nm thick *h*-CrTe film, instead of a bulk sample, is used in the measurements, our calculation has reproduced the experimental spectrum quit well and the MCD of *h*-CrTe is indeed quite different from that of ZB CrTe or $Zn_{1-x}Cr_xTe$. So, it is easy to identify the different magnetic precipitates in the samples by MCD analysis.

IV. CONCLUSION

The absorption and MCD spectra of $Zn_{1-x}Cr_xTe$ for $x=0.0625$, 0.25, and the end limit 1.0 are studied by *ab initio* calculations. The critical features of MCD are kept to be unchanged for $x \leqslant 0.25$ though additional MCD structures appear in the high doping case $x=0.25$ and 1.0 due to the large weight of transitions from Te p to Cr d bands. At *L*-CPs, our calculations reproduce very well the experimental MCD structure though at the absorption edge E_0, a positive MCD signal opposite to the measurement is obtained. The positive MCD signal at E_1 and the negative one at $E_1+\Delta_1$ indicate the p-d exchange interaction in $Zn_{1-x}Cr_xTe$ does exist and is FM. The calculated MCD spectrum of NiAs-type CrTe is also comparable with the experimental measurement and found to be different from that of $Zn_{1-x}Cr_xTe$. Our numerical results confirm that the MCD analysis is efficient in identifying the p-d exchange interaction in DMS and can be used for distinguishing the different phases of magnetic precipitates in the samples.

Note added in proof. Recently, we have become aware that the MCD spectrum measured for $Zn_{1-x}Cr_xTe$ ($x=0.12$) in Fig. 1(c) of Ref. 34 is a better comparison to our calculations, especially with regard to the broad positive MCD signal between the E_0 and E_1 points. As we have discussed, the MCD around E_1 and $E_1+\Delta_1$ is quite stable, while that around E_0 is very sensitive to the details in the samples. The significant difference of the measured broad MCD signal for $x=0.12$ and $x=0.2$ is not well understood at this point. More experimental measurements on various samples are needed to clarify this.

ACKNOWLEDGMENTS

The authors thank the staff of the Center for Computational Materials Science at IMR for their support and the use of the Hitachi SR8000/64 supercomputing facilities. H.W. acknowledges the valuable discussion with K. Ando.

*Corresponding author. Email address: hongming@imr.edu

[1] S. A. Wolf, D. D. Awschalom, R. A. Buhrman, J. M. Daughton, S. Von Molnár, M. L. Roukes, A. Y. Chtchelkanova, and D. M. Treger, Science **294**, 1488 (2001); Igor Žutić, Jaroslav Fabian, and S. Das Sarma, Rev. Mod. Phys. **76**, 323 (2004).

[2] M. E. Overberg, C. R. Abernathy, S. J. Pearton, N. A. Theodoropoulou, K. T. McCarthy, and A. F. Hebard, Appl. Phys. Lett. **79**, 3473 (2001).

[3] M. Hashimoto, Y. K. Zhou, M. Kanamura, and H. Asahi, Solid State Commun. **122**, 37 (2002); S. E. Park, H. J. Lee, Y. C. Cho, S. Y. Jeong, C. R. Cho, and S. Cho, Appl. Phys. Lett. **80**, 4187 (2002).

[4] Y. Matsumoto, M. Murakami, T. Shono, T. Hasegawa, T. Fukumura, M. Kawasaki, P. Ahmet, T. Chikyow, S. Koshihara, and H. Koinuma, Science **291**, 854 (2001); Y. Matsumoto, R. Takahashi, M. Murakami, T. Koida, X. J. Fan, T. Hasegawa, T. Fukumura, M. Kawasaki, S. Koshihara, and H. Koinuma, Jpn. J. Appl. Phys., Part 2 **40**, L1204 (2001); J. D. Bryan, S. M. Heald, S. A. Chambers, and D. R. Gamelin, J. Am. Chem. Soc. **126**, 11640 (2004).

[5] K. Ueda, H. Tabata, and T. Kawai, Appl. Phys. Lett. **79**, 988 (2001); P. Sati, R. Hayn, R. Kuzian, S. Régnier, S. Schäfer, A. Stepanov, C. Morhain, C. Deparis, M. Laügt, M. Goiran, and Z. Golacki, Phys. Rev. Lett. **96**, 017203 (2006).

[6] P. Sharma, A. Gupta, K. V. Rao, F. J. Owens, R. Sharma, R. Ahuja, J. M. O. Guillen, B. Johansson, and G. A. Gehring, Nat. Mater. **2**, 673 (2003).

[7] G. A. Medvedkin, T. Ishibashi, T. Nishi, K. Hayata, Y. Hasegawa, and K. Sato, Jpn. J. Appl. Phys., Part 2 **39**, L949 (2000).

[8] H. Saito, V. Zayets, S. Yamagata, and K. Ando, Phys. Rev. Lett. **90**, 207202 (2003).

[9] N. Ozaki, N. Nishizawa, S. Kuroda, and K. Takita, J. Phys.: Condens. Matter **16**, S5773 (2004).

[10] T. Zhao, S. R. Shinde, S. B. Ogale, H. Zheng, T. Venkatesan, R. Ramesh, and S. Das Sarma, Phys. Rev. Lett. **94**, 126601 (2005).

[11] K. Ando, Science **312**, 1883 (2006).

[12] J. K. Furdyna, J. Appl. Phys. **64**, R29 (1988).

[13] K. Ando, in *Magneto-Optics*, edited by S. Sugano and N. Kojima, Springer Series in Solid-State Science Vol. 128 (Springer, Berlin, 2000), Ch. 6.

[14] K. Ando, T. Hayashi, M. Tanaka, and A. Twardowski, J. Appl. Phys. **83**, 6548 (1998).
[15] K. Ando, Appl. Phys. Lett. **82**, 100 (2003).
[16] H. Saito, W. Zaets, R. Akimoto, K. Ando, Y. Mishima, and M. Tanaka, J. Appl. Phys. **89**, 7392 (2001).
[17] K. Ando and H. Munekata, J. Magn. Magn. Mater. **272-276**, 2004 (2004).
[18] K. Ando, H. Saito, Z. Jin, T. Fukumura, M. Kawasaki, Y. Matsumoto, and H. Koinuma, Appl. Phys. Lett. **78**, 2700 (2001); K. R. Kittilstved, W. K. Liu, and D. R. Gamelin, Nat. Mater. **5**, 291 (2006).
[19] K. Ando, cond-mat/0208010 (unpublished); K. Ando, H. Saito, V. Zayets, and M. C. Debnath, J. Phys.: Condens. Matter **16**, S5541 (2004).
[20] H. Weng, J. Dong, T. Fukumura, M. Kawasaki, and Y. Kawazoe, Phys. Rev. B **73**, 121201(R) (2006).
[21] P. Blaha, K. Schwarz, G. K. H. Madsen, D. Kvasnicka, and J. Luitz, WIEN2K, An Augmented Plane Wave+Local Orbitals Program for Calculating Crystal Properties (Karlheinz Schwarz, Techn. Universität, Wien, Austria, 2001).
[22] J. P. Perdew, K. Burke, and M. Ernzerhof, Phys. Rev. Lett. **77**, 3865 (1996).
[23] D. D. Koelling and B. N. Harmon, J. Phys. C **10**, 3107 (1977); A. H. MacDonald, W. E. Pickett, and D. D. Koelling, *ibid.* **13**, 2675 (1980).
[24] H. Ebert, Rep. Prog. Phys. **59**, 1665 (1996).
[25] H. Weng, Y. Kawazoe, and J. Dong, Phys. Rev. B **74**, 085205 (2006).
[26] J. Kuneš, P. Novák, M. Diviš, and P. M. Oppeneer, Phys. Rev. B **63**, 205111 (2001).
[27] E. Ghahramani, D. J. Moss, and J. E. Sipe, Phys. Rev. B **43**, 9700 (1991).
[28] R. M. Dreizler and E. K. U. Gross, *Density Functional Theory, An Approach to the Quantum Many-Body Problem* (Springer-Verlag, Berlin, 1990).
[29] W. H. Xie and B. G. Liu, J. Appl. Phys. **96**, 3559 (2004); Q. Wang, Q. Sun, P. Jena, and Y. Kawazoe, *ibid.* **97**, 043904 (2005).
[30] A. K. Bhattacharjee, Phys. Rev. B **49**, 13987 (1994); P. Kacman, Semicond. Sci. Technol. **16**, R25 (2001).
[31] B. E. Larson, K. C. Hass, H. Ehrenreich, and A. E. Carlsson, Phys. Rev. B **37**, 4137 (1988); M. Wierzbowska, D. Sanchez-Portal, and S. Sanvito, *ibid.* **70**, 235209 (2004).
[32] J. Szczytko, W. Mac, A. Stachow, A. Twardowski, P. Becla, and J. Tworzydlo, Solid State Commun. **99**, 927 (1996); A. Twardowski, Mater. Sci. Eng., B **63**, 96 (1999); J. Szczytko, W. Mac, A. Twardowski, F. Matsukura, and H. Ohno, Phys. Rev. B **59**, 12935 (1999); J. Szczytko, W. Bardyszewski, and A. Twardowski, *ibid.* **64**, 075306 (2001); T. Hartmann, S. Ye, P. J. Klar, W. Heimbrodt, M. Lampalzer, W. Stolz, T. Kurz, A. Loidl, H. A. Krug von Nidda, D. Wolverson, J. J. Davies, and H. Overhof, *ibid.* **70**, 233201 (2004).
[33] S. Picozzi, A. Continenza, M. Kim, and A. J. Freeman, Phys. Rev. B **73**, 235207 (2006).
[34] H. Saito, V. Zayets, S. Yamagata, and K. Ando, J. Appl. Phys. **93**, 6796 (2003).